Molecular Biology of the Cell
Vol. 13, 1819–1831, June 2002

The Small GTPase Rab13 Regulates Assembly of Functional Tight Junctions in Epithelial Cells

Anne-Marie Marzesco,*† Irene Dunia,† Rudy Pandjaitan,* Michel Recouvreur,‡ Daniel Dauzonne,§ Ennio Lucio Benedetti,‡ Daniel Louvard,* and Ahmed Zahraoui*‖

*Laboratory of Morphogenesis and Cell Signaling, UMR144 Centre National de la Recherche Scientifique (CNRS), Institut Curie, Paris; ‡Institut Jacques Monod, CNRS, Universite Paris 6–7, Paris; and §UMR176 CNRS, Institut Curie, Paris, France

Submitted December 17, 2001; Revised February 8, 2002; Accepted March 8, 2002
Monitoring Editor: Keith Mostov

Junctional complexes such as tight junctions (TJ) and adherens junctions are required for maintaining cell surface asymmetry and polarized transport in epithelial cells. We have shown that Rab13 is recruited to junctional complexes from a cytosolic pool after cell–cell contact formation. In this study, we investigate the role of Rab13 in modulating TJ structure and functions in epithelial MDCK cells. We generate stable MDCK cell lines expressing inactive (T22N mutant) and constitutively active (Q67L mutant) Rab13 as GFP-Rab13 chimeras. Expression of GFP-Rab13Q67L delayed the formation of electrically tight epithelial monolayers as monitored by transepithelial electrical resistance (TER) and induced the leakage of small nonionic tracers from the apical domain. It also disrupted the TJ fence diffusion barrier. Freeze-fracture EM analysis revealed that tight junctional structures did not form a continuous belt but rather a discontinuous series of stranded clusters. Immunofluorescence studies showed that the expression of Rab13Q67L delayed the localization of the TJ transmembrane protein, claudin1, at the cell surface. In contrast, the inactive Rab13T22N mutant did not disrupt TJ functions, TJ strand architecture nor claudin1 localization. Our data revealed that Rab13 plays an important role in regulating both the structure and function of tight junctions.

INTRODUCTION

The plasma membrane of epithelial cells displays apical and basolateral domains with distinct composition and properties. The maintenance of the cell surface asymmetry requires junctional complexes such as, tight junctions (TJ), adherens junctions, and desmosomes. TJ act as a selective barrier restricting the diffusion of ions and solutes across the paracellular space (gate function). They also form a "fence" preventing lateral diffusion of plasma membrane proteins and lipids. Freeze-fracture electron microscopy (EM) revealed that the TJ was composed of linear rows that were tightly connected to similar rows on adjacent cell membranes. Much work has been devoted to understanding the molecular architecture of TJ. Occludin and claudins, two transmembrane proteins associated with TJ strands, are thought to seal the paracellular space and to generate a series of regulated channels within TJ membranes for the passage of ions and small molecules (Tsukita and Furuse, 1999). Exactly, how TJ assemble is still a matter of debate. Several peripheral membrane proteins such ZO-1, ZO-2, and ZO-3 are thought to link occludin and claudins to the underlying actin cytoskeleton. ZO proteins contain 3 PDZ and 1 SH3 domains that may recruit and cluster proteins to TJ (Cordenonsi *et al.*, 1999; Itoh *et al.*, 1999; Wittchen *et al.*, 1999; Balda and Matter, 2000). However, it remains to be determined how these protein complexes may control both the dynamics of TJ assembly and the TJ barrier functions. Adherens junctions are positioned below TJ and consist of adhesion and signaling molecules. E-cadherin, a basolateral transmembrane protein, plays a key role in the formation and maintenance of junctional complexes (Gumbiner *et al.*, 1988). However, expression of a dominant negative mutant of E-cadherin in MDCK cells did not affect tight junctions (Troxell *et al.*, 2000). The mechanisms that regulate the as-

Article published online ahead of print. Mol. Biol. Cell 10.1091/mbc.02–02–0029. Article and publication date are at www.molbiolcell.org/cgi/doi/10.1091/mbc.02–02–0029.

‖ Corresponding author. E-mail address: zahraoui@curie.fr.
† Present address: Max Planck Institute of Molecular Cell Biology and Genetics, Dresden, Germany.

Abbreviations used: MDCK, Madin-Derby Canine Kidney; TJ, tight junction; TER, transepithelial electrical resistance; EM, electron microscopy; EF, exoplasmic fracture face; PF, protoplasmic fracture face; WT, wild-type.

sembly and maintenance of TJ and adherens junctions are not well understood.

Previous studies suggest that junctional complexes may constitute a specific targeting site on the lateral plasma membrane for delivery of specialized cargo vesicles (Louvard, 1980). This proposal is supported by the finding that many proteins involved in membrane trafficking are concentrated in cell–cell junctions (Zahraoui *et al.*, 2000). In MDCK cells, antibodies against Sec8, an exocyst subunit, inhibit vesicles delivery to the basolateral membrane (Grindstaff *et al.*, 1998). Three small GTPases, Rab3b, Rab8, and Rab13, are localized in cell–cell contacts in epithelial cells (Huber *et al.*, 1993; Weber *et al.*, 1994; Zahraoui *et al.* 1994). Rab proteins are involved in the regulation of different steps of exocytic and endocytic pathways (Schimmoller *et al.*, 1998; Chavrier and Goud, 1999; Zerial and McBride, 2001). Although the exact role of Rab proteins is still unclear, they may control the assembly of protein complexes involved in various cellular processes including vesicle movement and fusion or actin organization (Stenmark *et al.*, 1995; Kato *et al.*, 1996; Peränen *et al.*, 1996; Ren *et al.*, 1996; Echard *et al.*, 1998; Nielsen *et al.*, 1999; White *et al.*, 1999). Recently, we have found that Rab13 is recruited to cell–cell contacts at an early stage of assembly of junctional complexes (Sheth *et al.*, 2000), suggesting that Rab13 may be a good candidate for regulating the assembly cell–cell junctions. In this study, we investigate the role of Rab13 in TJ functions. The expression of the constitutively active form of GFP-Rab13 (Q67L mutant) affected TER and increased the paracellular flux of small tracers. It also induced a disorganization of TJ strand networks and a delay in the localization of the TJ transmembrane protein, claudin1. In contrast, the inactive GFP-Rab13T22N mutant reduced paracellular permeability and had no effect on TJ strand organization and claudin1 localization. Our results provide a new insight into the role of Rab13 protein in regulating TJ assembly.

MATERIALS AND METHODS

Antibodies

The mouse mAb anti-GFP was purchased from Roche (Roche Diagnostics GmbH, Mannheim, Germany). The monoclonal antigp58 and gp-114 antibodies were kindly provided by K. Simons (Max Planck Institute, Dresden, Germany). The rat monoclonal raised against ZO-1 (R40.76) was used (Anderson *et al.,* 1989). The polyclonal rabbit antioccludin and anticlaudin-1 were purchased from Zymed (Zymed Laboratories, Inc., South San Francisco, CA). The affinity-purified goat anti-mouse, or anti-rat or anti-rabbit IgG conjugated to either TRITC or Cy5 were purchased from Jackson ImmunoResearch Laboratories, Inc.(West Grove, PA).

Mutagenesis and Transfection

Dominant negative (T22N) and the constitutively active (Q67L) Rab13 mutants were generated from Rab13 cDNA using site-directed mutagenesis kit (Stratagene, La Jolla, CA), and 5′ TCGGGGGTGGGCAAGAATTGTCTGATCATTCGCTT-3′ and 5′-GGGACACGGCTGGCCTAGAGCGGTTCAAGACAATA-3′ oligonucleotides respectively. An *Eco*RI site was introduced by PCR upstream of the ATG codon of Rab13. *Eco*RI-*Bam*HI inserts encoding Rab13WT, Rab13T22N, and Rab13Q67L were fused to the C terminus of the enhanced green fluorescent protein (GFP) and cloned into pGFP-C3 vector (Clontech Inc., Palo Alto, CA). All constructions were verified by sequencing. Stable MDCK cell lines expressing GFP-Rab13WT, GFP-Rab13T22N, GFP-Rab13Q67L, and the mock MDCK expressing GFP were generated by transfection using the effectene transfection reagent according to the manufacturer instructions (Qiagen GmbH, Hilden, Germany). Positive clones were selected and cloned in the same medium supplemented with 1 mg/ml G418 (Life Technologies, Eggenstein, Germany). The expression of GFP, GFP-Rab13 WT, T22N, and Q67L mutants was checked by immunobloting and by immunofluorescence using a monoclonal anti-GFP antibody. Two independent clones of GFP-Rab13T22N and GFP-Rab13Q67L were grown up and subsequently analyzed.

Cell Culture and Growth

MDCK cells (strain II) were grown in DMEM supplemented with 10% fetal calf serum, 2 mM glutamine, 100 U/ml penicillin, and 10 mg/ml streptomycin. The cultures were incubated at 37°C under a 10% CO_2 atmosphere.

In all our experiments, 600,000 cells/cm^2 were plated onto polycarbonate filters (0.4-μm pore size and 12-mm diameter; Transwell; Costar Corp., Cambridge, MA) as instant confluent monolayers and grown for 3 d. The expression of the ectopic proteins was induced by treatment with 10 mM sodium butyrate for 15 h before analysis. Parental MDCK and MDCK expressing GFP alone were also treated with 10 mM sodium butyrate. Stable transfected clones were maintained under selection in 500 μg/ml G418. To remove extracellular calcium, confluent MDCK cells were rinsed three times in low calcium medium (S-MEM) and incubated with S-MEM for 15 h. Cells were then rinsed with normal DMEM, incubated in DMEM for 0, 2, 4, and 15 h, and analyzed by immunofluorescence.

Immunofluorescence Microscopy

Parental or transfected MDCK cells were washed with PBS containing 1 mM $CaCl_2$, 0.5 mM $MgCl_2$ and fixed with 2% paraformaldehyde in PBS for 15 min. The free aldehyde groups were quenched for 15 min with 50 mM NH_4Cl in PBS. Cells were then permeabilized with 0.5% Triton X-100 in PBS for 15 min and then blocked in PBS buffer containing 0.5% Triton X-100 and 0.2% BSA. All subsequent incubations with antibodies and washes were performed with this buffer. Cells were incubated overnight at 4°C with the primary antibodies, rinsed three times for 10 min with the blocking buffer, and then incubated with affinity-purified secondary antibodies raised in goat and conjugated to TRITC or Cy5. After 45 min the filters were washed three times more with the same buffer and three times with PBS. The samples were mounted in 50% glycerol-PBS and analyzed with a Leica SP2 confocal laser scanning microscope (Leica Microscopy and Systems GmbH, Mannheim, Germany).

Measurement of Transepithelial Electrical Resistance

MDCK cells were plated on filters as instant confluent monolayers. TER of filters (12-mm diameter) were determined by applying an AC square wave current of 20 μA at 12.5 Hz and measuring the voltage deflection with a Ag/AgCl electrode using an Epithelial VoltOhmMeter (EVOM; World Precision Instruments, Sarasota, FL). TER values were determined by subtracting the contribution of filter and medium.

Paracellular Flux Assay

Paracellular permeability was measured using three different tracers: [^{3}H]mannitol (182 Da), 4 kDa FITC-Dextran, and 40 kDa FITC-Dextran. Cells were grown on filters to confluency for 3 d, and the monolayers were treated overnight with sodium butyrate. The stock solution of FITC-Dextran (20 mg/ml; Sigma-Aldrich Chemie GmbH, Deisenhofen, Germany) was dialyzed against P buffer (10 mM HEPES, pH 7.4, 1 mM sodium pyruvate, 10 mM glucose, 3 mM $CaCl_2$, 145 mM NaCl) and diluted to 2 mg/ml in P buffer before the

assay. We measured paracellular diffusion from the apical to the basolateral domain. The assay was started by replacing the basolateral medium with 500 μl of P buffer and the apical culture medium with 250 μl of solution containing 2 mg/ml of 4K FITC-Dextran or 40K FITC-Dextran. Monolayers were incubated at 37°C for 3 h, and the basal chamber media was collected. FITC-Dextran was measured with a fluorometer (excitation: 392 nm; emission: 520 nm; Perkin Elmer-Cetus Applied Biosystems, Inc., Überlingen, Germany). Paracellular flux of [^{3}H]mannitol was measured as described (Balda *et al.*, 1993). Briefly, we added to the upper chamber 500 μl of tissue culture medium containing 1 mM mannitol and 4 μCi/ml [^{3}H]mannitol. After 1 h at 37°C, aliquots were removed, and radioactivity was counted in a liquid scintillation counter (Wallac Oy, Turku, Finland).

Freeze-fracture Electron Microscopy and Immunolabeling

MDCK cells were plated in 10-cm diameter tissue culture plates and grown to confluency for 3 d. For conventional freeze-fracture, cells were fixed in 2% glutaraldehyde in 0.1 M cacodylate buffer, pH 7.4, for 30 min at room temperature. Cells were scraped from the substrate with a plastic cell scraper and infiltrated with 30% glycerol for 2 h at 4°C. Freeze-fracture was performed at −130°C in a Balzers freeze-fracture 301 or 400 unit (Balzers, Liechtenstein; Fujimoto, 1997; Dunia *et al.*, 2001). Replicas were examined using a Philips CM12 electron microscope (Eindhoven, The Netherlands).

Diffusion of BODIPYR6G-Sphingosylphosphorylcholin

BodipyR6G-sphingosylphosphorylcholin was prepared by reacting BodipyR6G SE (the succinimidyl ester of the 4,4-difluoro-5-phenyl-4-bora-3a,4a-diaza-*s*-indacene-3-propionic acid purchased from Molecular Probes Inc., Eugene, OR) with sphingosylphosphorylcholin (Sigma-Aldrich Chimie GmbH) as follows: a suspension of sphingosylphosphorylcholin (10.6 mg, 0.0228 mmol) in anhydrous dimethylformamide (5 ml) was placed, under inert atmosphere, in a 10-ml round-bottom flask fitted with a magnetic bar. BodipyR6G SE (10 mg, 0.0228 mmol) was added, in one portion, to the mixture, and the stirring was continued for 48 additional hours at room temperature. Removal of the solvent at 50°C under reduced pressure provided *N*-(4,4-difluoro-5-phenyl)-4-bora-3a,4a-diaza-*s*-indacene-3-propionyl)sphingosylphosphorylcholin (16.7 mg, 93% yield) as a dark powder: Mass Spectrum-FAB: *m/z* 787 $(M + H)^+$, 809 $(M + Na)^+$. This fluorescent lipid was thus obtained satisfactorily pure for subsequent utilization without further purification as judged by TLC on silica gel (eluent: dichloromethane/methanol/triethylamine: 50/49/1).

BODIPYR6G-sphingosylphosphorylcholin/BSA complexes were obtained by adding 400 μl of BODIPYR6G-sphingosylphosphorylcholin stock solution (1 mM in DMSO) to 10 ml of BSA solution (0.8 mg/ml defatted BSA in 10 mM HEPES, pH 7.4, 145 mM NaCl). To label the cells, monolayers were washed twice with cold P buffer, then 250 μl of fluorescent lipid/BSA was added to the apical chamber, and the cells were incubated for 10 min on ice. Cells were first washed four times with P buffer and then either left on ice for 1 h or directly mounted in P buffer. For mounting, double-sided tape on each side of the microscope slide was used to support the coverslip and to avoid pressure on the sample. The lateral diffusion of the fluorescent lipid was analyzed within the first 10 min by confocal microscopy.

Immunoblotting

MDCK cells expressing GFP, GFP-Rab13T22N, and GFP-Rab13Q67L were grown on 10-cm-diameter culture plates for 3 d and treated with 10 mM sodium butyrate for 15 h. They were extracted in 1 ml of 0.5% Triton X-100 (vol/vol), 10 mM Tris-HCl, pH 7.6, 120 mM NaCl, 25 mM KCl, 1.8 mM $CaCl_2$, 1 mM sodium vanadate, 50 mM NaF, 1 mM pefabloc, and a mixture of protease inhibitors (1 μg/ml pepstatin, 10 μg/ml leupeptin, and aprotinin) on a rocker platform for 20 min at 4°C. Solubilized materials (Triton X-100 soluble) were recovered by pelleting at 18,500 × *g* for 15 min at 4°C. Pellets (Triton X-100 insoluble) were dissolved in 250 μl of the same buffer containing 1% SDS at 100°C. Supernatants were adjusted to 1% SDS and protein concentration was determined using the Bio-Rad protein assay kit (Bio-Rad laboratories, Hercules, CA). Equal amounts of Triton X-100 soluble (S) and insoluble (P) pools were separated by SDS-PAGE and transferred electrophoretically to nitrocellulose filters. The upper and lower parts of the filters were probed with antioccludin and anticlaudin1 antibodies respectively. After blotting, soluble and insoluble occludin and claudin1 protein bands were quantified using the Scion image program (NIH image, Rockville, MD) and Microsoft Excel software (Redmond, WA). The insoluble (P)/soluble (S) ratio was calculated (mean + SEM).

RESULTS

Expression of GFP-Rab13 in MDCK Cells

Rab proteins cycle between GDP-bound inactive and GTP-bound active states. To investigate the role of Rab13 in TJ function, we generated two mutants, Rab13T22N and Rab13Q67L. In Ras and other Rab proteins, the equivalent of Q67L mutant is deficient in GTP hydrolysis, so it cannot undergo catalytic cycling to GDP-bound form and remains bound to its effectors on target membranes; therefore, this mutant is considered as an activated form of the GTPase. The Rab13T22N mutant is expected to be inactive. The corresponding mutation in Ras and Rab has a lower affinity for GTP than for GDP. It also appears to sequester the exchange factor thereby inhibiting the function of the endogenous protein. Rab13 wild-type (WT), Rab13T22N, and Rab13Q67L mutants fused to the C terminus of the enhanced green fluorescent protein (GFP) were expressed in stably transfected MDCK cells. Unfortunately, our anti-Rab13 antibodies did not detect the endogenous protein, we could not compare the level of expression, nor the localization of the exogenic GFP-Rab13 to that of the endogenous protein. Immunoblot analysis using anti-GFP antibody revealed that the expression of the ectopic GFP-Rab13 proteins was very weak, in particular for the GFP-Rab13T22N protein (Figure 1A). This prompted us to treat the cells with 10 mM sodium butyrate for 15 h to stimulate the expression of the transfected cDNAs. Under these conditions, the sodium butyrate treatment did not cause changes in TJ structure or functions (Balda *et al.*, 1996; this work). Compared with nontreated cells, the sodium butyrate treatment led to a 1.5-fold increase in the amount of GFP, GFP-Rab13 WT, and GFP-Rab13Q67L proteins and a 6-fold increase in the expression of GFP-Rab13T22N protein (Figure 1A). Except for the TER experiments, the expression of the ectopic proteins was induced for 15 h with 10 mM sodium butyrate before analysis. Parental MDCK and MDCK expressing GFP alone were also treated with 10 mM sodium butyrate. We checked that this treatment had no effect on the targeting of GFP-Rab13.

In isolated islets of differentiating MDCK cells, GFP-Rab13 WT and Q67L were found in the perinuclear region and in cell–cell contacts where junctional complexes developed with neighboring cells. GFP-Rab13 was absent from the edges of cells devoid of junctional complexes. The GFP-Rab13T22N mutant was observed on cytoplasmic structures

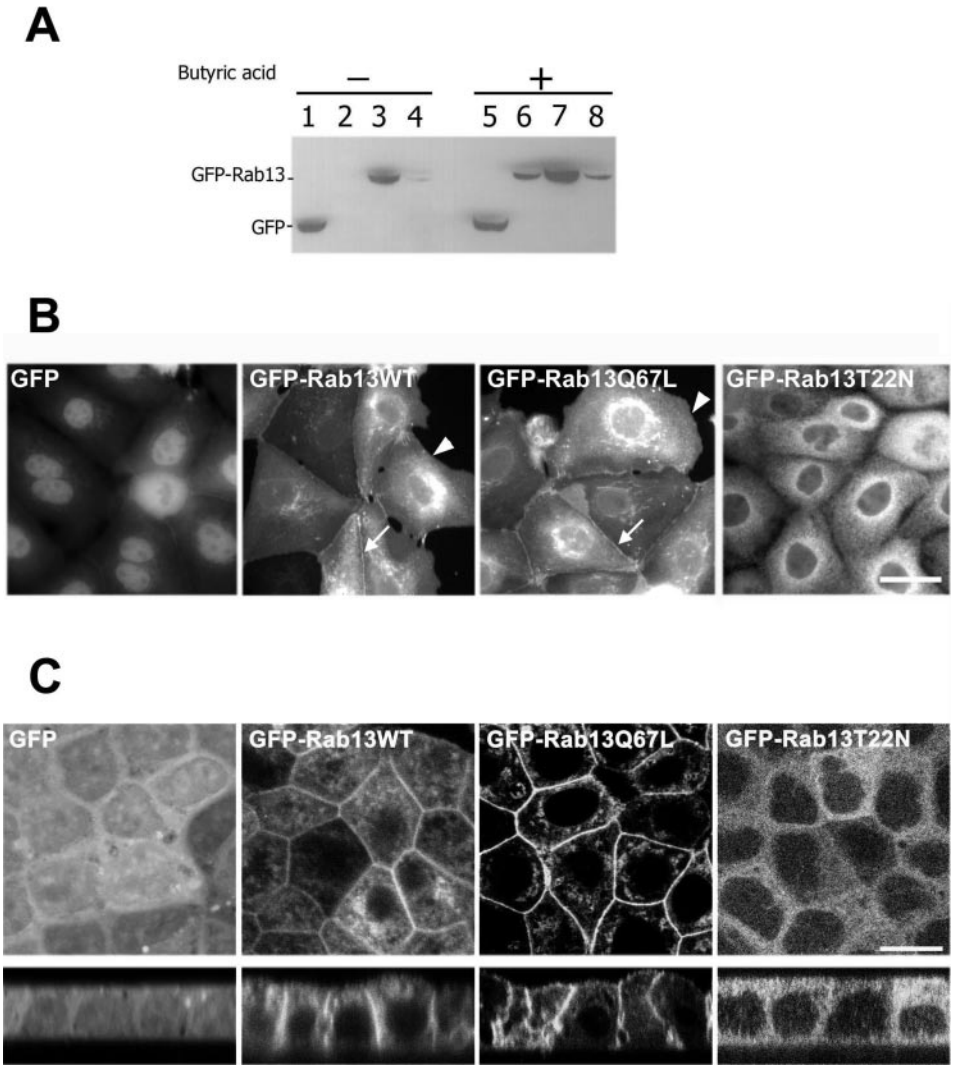

Figure 1. Expression of GFP-Rab13 proteins in stably transfected MDCK cells in presence (+) or absence (−) of butyric acid. (A) Proteins in equal amounts of cell extracts prepared from cells expressing GFP (lanes 1 and 5), GFP-Rab13T22N (lanes 2 and 6), GFP-Rab13Q67L (lanes 3 and 7), and GFP-Rab13WT (lanes 4 and 8) were separated by SDS-PAGE and transferred to nitrocellulose filters. The filter was probed with monoclonal anti-GFP antibody. (B) Immunofluorescence localization of GFP-Rab13 in stably transfected MDCK cells. Cells expressing GFP, GFP-Rab13T22N, or GFP-Rab13Q67L were grown for 1 d to form small islets of differentiating MDCK cells. After sodium butyrate treatment, cells were processed for immunofluorescence. Arrowheads indicate the periphery of cells devoid of junctional complexes. Cells were viewed with a Leica microscope and photographed. GFP-Rab13 WT and Q67L proteins are found in the perinuclear region and in regions of cell that are in contact with neighboring cells (arrows). Note the absence of GFP-Rab13 WT and Q67L staining from the edges of cells devoid of cell–cell junctions (arrowheads). (C) Cells expressing GFP, GFP-Rab13wt, GFP-Rab13T22N, or GFP-Rab13Q67L were grown on Transwell filters for 3 d. After sodium butyrate treatment and fixation, cells were processed for confocal laser scanning microscopy. Shown are one (*x*-*y*) focal plane taken at the tight junction level and a *z*-section. GFP-Rab13 wild-type and GFP-Rab13Q67L constructs were targeted to the lateral membrane including junction's area. Bar, 10 μm

distributed throughout the cells. GFP alone was found in the nucleus and as a diffuse staining in the cytoplasm (Figure 1B). These results indicated that the recruitment of GFP-Rab13 to the plasma membrane required cell–cell contact formation. In confluent cells, GFP-Rab13WT and Rab13Q67L mutant were distributed along the lateral plasma membrane including tight junctions as well as on cytoplasmic structures. No labeling either due to binding to apical or basal plasma membranes could be detected. GFP-Rab13T22N was observed on cytoplasmic structures distributed throughout the cells (Figure 1C). To ascertain whether the presence of GFP tag may have disturbed the localization of Rab13, we transiently expressed a carboxy terminus VSV-G–tagged Rab13 T22N and Q67L mutants in MDCK cells. Similarly to GFP-Rab13 constructs, we found that VSV-Rab13Q67L localized to the plasma membrane and VSV-Rab13T22N to cytoplasmic structures (supplementary material). Moreover, we also examined the distribution of an other GFP-tagged protein Rab8, which shares high amino acid identity with Rab13 (Zahraoui *et al.*, 1994) and is also associated with tight junctions in MDCK cells (Huber *et al.*, 1993). GFP-Rab8Q67L localized to perinuclear region and to the plasma membrane (supplementary material) was consistent with the localization of endogenous Rab8 in MDCK cells (Huber *et al.*, 1993). These data suggest that the GFP tag did not affect the distribution of Rab proteins in MDCK cells.

Expression of GFP-Rab13Q67L Delays the Formation of Electrically Tight Epithelial Monolayers

Zonula occludens tightly seal the apex of adjacent cells to form an epithelial sheet. The transepithelial electrical resistance (TER) can be used to monitor the tightness of the seal between neighboring cells. Because the recruitment of Rab13 to the apicolateral junctional complex occurred at an early stage in the assembly of TJ (Zahraoui *et al.*, 1994; Sheth *et al.*, 2000), we postulated that it might be involved in TJ sealing. Therefore, we measured TER over a 120-h time period of parental MDCK, GFP, GFP-Rab13WT, GFP-Rab13T22N, and

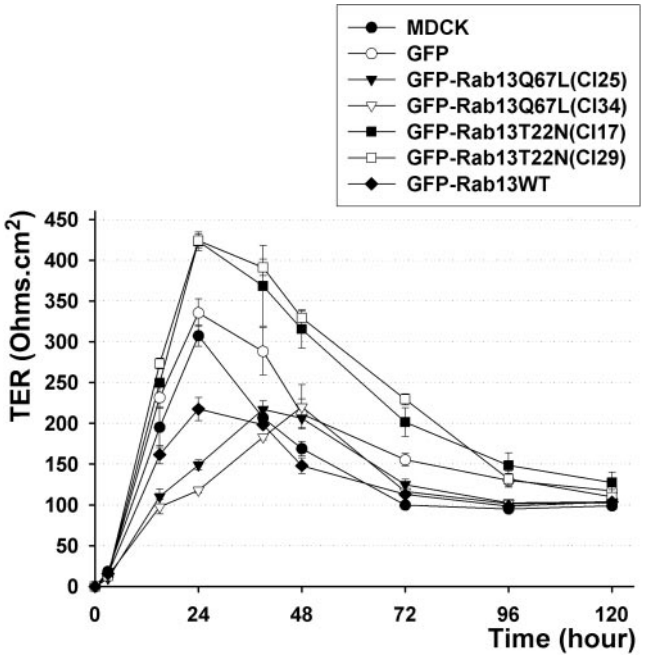

Figure 2. TER development in MDCK cells and MDCK expressing GFP, GFP-Rab13WT, GFP-Rab13T22N, or GFP-Rab13Q67L. Cells were plated on filters as instant confluent monolayers (0 min). TER was measured at different times >120 h, and background resistance of empty filters was subtracted. Average values are given ± SEM of each cell clone as derived from four independent determinations and performed in duplicate. In these experiments, cells were not treated with sodium butyrate. At the end of each experiments, the integrity of the monolayer was checked by ZO-1 staining. The results of two independent clones of GFP-Rab13T22N and GFP-Rab13Q67L cells are shown. We measured the TER of a third independent GFP-Rab13Q67L clone, which exhibited similar TER development than the two presented here.

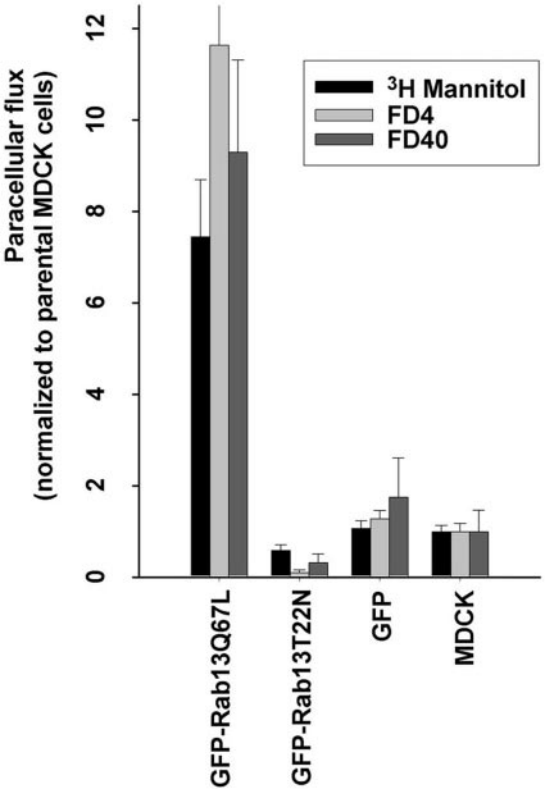

Figure 3. Paracellular flux of nonionic tracers in MDCK and in GFP-Rab13-transfected cells. Parental MDCK cells and cells expressing GFP, GFP-Rab13WT, GFP-Rab13T22N, or GFP-Rab13Q67L were plated as instant confluent monolayers and grown for 3 d. Cells were treated with sodium butyrate for 15 h. Paracellular flux of [^{3}H]mannitol, 4 kDa FITC-Dextran (FD4), and 40 kDa FITC-Dextran (FD40) was measured in the apical to basolateral direction. The amount of tracer diffusion is normalized to parental MDCK cells. The data of three independent experiments performed in duplicate are reported as the mean ± SEM

GFP-Rab13Q67L cells grown on filters (Figure 2). Because the same number of cells was plated per filter, the TER from different stable cell lines could be compared. Parental MDCK and cells expressing GFP showed a rapid increase in TER that reached 300 $\Omega \times cm^2$ by 24 h. In cells expressing GFP-Rab13T22N, TER reached 400 $\Omega \times cm^2$ by 24 h. In contrast, cells expressing the active GFP-Rab13Q67L exhibited a significant delayed TER development. TER developed slowly and reached a maximal value of 200 $\Omega \times cm^2$ only by 48 h. Similar alteration of TER recovery was seen in GFP-Rab13WT cells; although the effect was less pronounced than in GFP-Rab13Q67L cells, TER value reached 200 $\Omega \times cm^2$ by 24 h. This effect was expected because the overexpression of many RabWT proteins has been shown to have an effect that is similar to GTP-bound forms of Rab proteins (Bucci *et al.*, 1992; Peränen *et al.*, 1996; White *et al.*, 1999). After the peak, all cell lines recovered a similar steady state TER of 100–150 $\Omega \times cm^2$ by 72–96 h. The TER of three independent Q67L clones was measured. These clones exhibited similar TER development. This excluded the possibility that the TER lag found in MDCK expressing GFP-Rab13Q67L mutant was due to clonal variation. These results indicate that the TER delay observed in GFP-Rab13Q67L-expressing cells was specific and that the expression of the constitutively active GFP-Rab13Q67L mutant delayed the formation of electrically tight epithelial monolayers. They also indicate that the effect of GFP-Rab13 occurred during TJ assembly.

Active Rab13 Disrupts TJ Gate Function for Nonionic Molecules

TJ also act as a selective diffusion barrier for nonionic molecules. We examined whether Rab13 mutants could affect the diffusion of three nonionic tracers through the paracellular space: [^{3}H] mannitol (182Da), 4 kDa FITC-Dextran, and 40 kDa FITC-Dextran (Figure 3). In confluent MDCK and in cells expressing GFP, a small amount of these tracers diffused across the monolayer of cells. When cells expressing GFP-Rab13Q67L were analyzed, they showed a higher amount of paracellular diffusion of the three tracers. Compared with control cells, the expression of GFP-Rab13Q67L induced an 8-fold increase in the paracellular permeability of [^{3}H]mannitol and a 10- to 12-fold increase in the diffusion

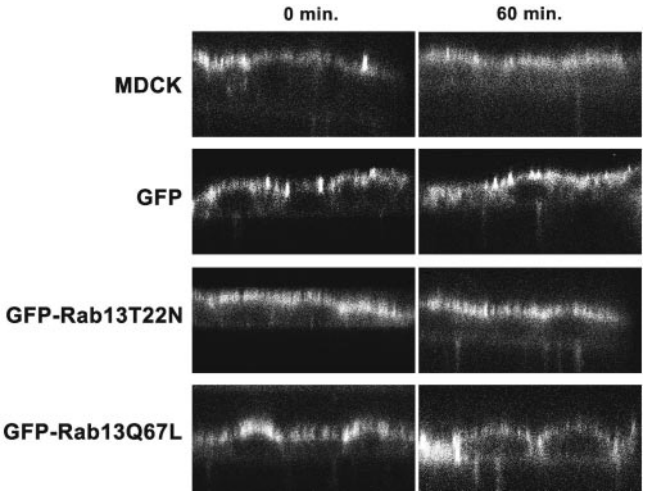

Figure 4. Diffusion of BODIPY-sphingosylphosphorylcholin/BSA complex from the apical to the lateral membrane in MDCK cells and in cells expressing GFP, GFP-Rab13T22N, and GFP-Rab13Q67L. Cells were grown on Transwell filters for 3 d and treated with sodium butyrate for 15 h. Fluorescent lipid/BSA was loaded to the apical surface for 10 min at 0°C, washed four times in P buffer (see MATERIAL AND METHODS), and either immediately processed for confocal microscopy (0 min) or left for an additional 60 min on ice (60 min). The lateral diffusion of the fluorescent lipid was then determined by *z*-sectioning on a confocal microscope. Bar, 10 μm.

of 4- and 40-kDa FITC-Dextran (Figure 3). In monolayers expressing the inactive GFP-Rab13T22N, the diffusion of the three tracers was reduced compared with that of control cells. We conclude that the expression of the GFP-Rab13Q67L mutant induced the leakage of small nonionic tracers from the apical domain.

Involvement of Rab13 in Tight Junction Fence Function

In addition to its gate function, TJ provide a physical fence for free diffusion of lipids and proteins in the outer leaflet of the plasma membrane between apical and basolateral domains. To examine whether the expression of active Rab13 affected the fence function of TJ, BODIPY-sphingosylphosphorylcholin/BSA was applied for 10 min at 4°C to the apical surface of butyrate-treated cell monolayers grown on filters. After washing, the diffusion of BODIPY-sphingosylphosphorylcholin/BSA was either immediately analyzed by confocal microscopy or analyzed after 60 min of incubation. The confocal *x*-*z* sections (Figure 4) show the distribution of membrane-labeled BODIPY-sphingosylphosphorylcholin/BSA in control cells and in Rab13 mutants. In cells expressing GFP or GFP-Rab13T22N mutant and in MDCK cells, the fluorescent lipid was confined to the apical domain at both 0 and 60 min. No lateral staining was detected. However, in MDCK expressing GFP-Rab13Q67L, BODIPY-sphingosylphosphorylcholin/BSA was not restricted after 60 min to the apical membrane but diffused across the TJ and stained the lateral membrane. When these cells were analyzed immediately after labeling with the lipid, BODIPY-sphingosylphosphorylcholin/BSA labeled only the apical membrane, indicating that BODIPY-sphingosylphosphorylcholin/BSA leakage after 60 min could not have resulted from an increase in the paracellular pathway.

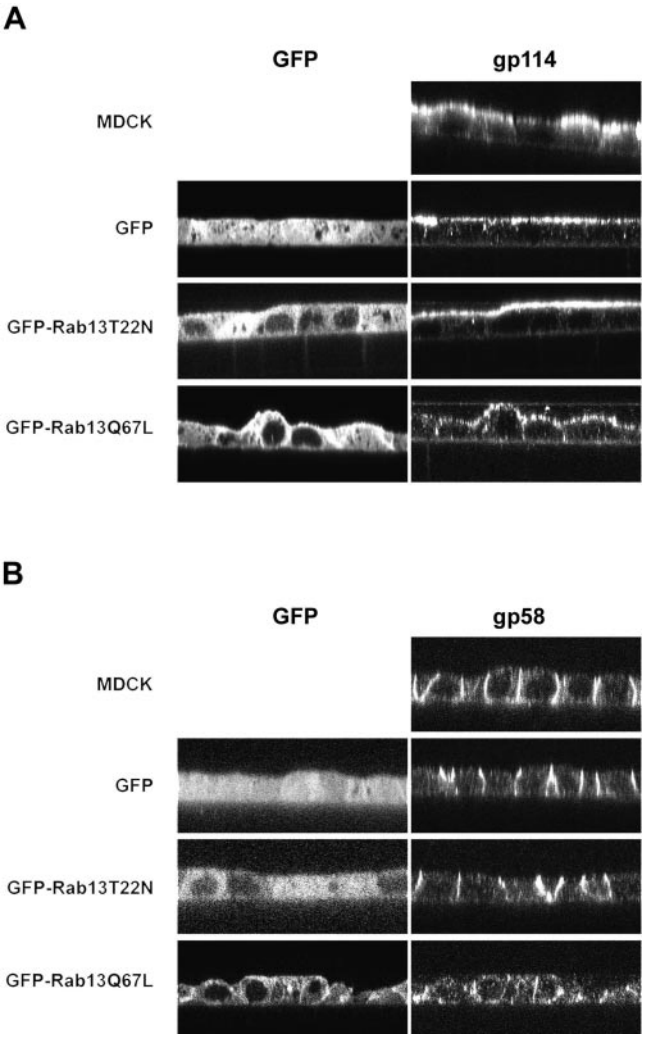

Figure 5. Distribution of the apical (A) gp114 and the basolateral (B) gp58 membrane proteins. Parental MDCK cells and cells expressing GFP, GFP-Rab13T22N, or GFP-Rab13Q67L were grown on Transwell filters for 3 d. Monolayers were fixed, permeabilized, and stained either with mouse monoclonal anti-gp114 or anti-gp58 antibodies. The primary antibodies were visualized with goat anti-mouse Cy5. Cells were then analyzed by confocal microscopy. The *z*-sections show the localization of gp58 and gp114 in transfected and untransfected MDCK cells. Bar, 10 μm.

We next investigated whether the expression of Rab13 mutants interfered with the polarized distribution of gp114 and gp58, two membrane proteins that are targeted and restricted to the apical and basolateral domains, respectively. Figure 5 shows the *x*-*z* confocal sections of gp114 and gp58. In control cells (MDCK and MDCK-expressing GFP) as well as in cells expressing GFP-Rab13T22N mutant, gp114 and gp58 proteins were correctly localized. In GFP-Rab13Q67L cells, gp114 and gp58 staining was not specifically restricted to apical and basolateral membrane domains,

respectively, although the cell morphology was altered. Both gp114 and gp58 staining was still detected in the cytoplasm and also on the lateral membrane for gp114. Taken together, the results indicate that the expression of the activated form of GFP-Rab13 altered the distribution of apical and basolateral membrane proteins.

Active Rab13 Induces Dramatic Changes in TJ Strand Organization

Given the effect of the activated form of Rab13 on TJ gate and fence function, we next asked whether this Rab13 mutant could affect the TJ structure. We examined by freeze-fracture EM the TJ strand organization, which provides a measure of TJ integrity. Freeze-fracture analysis of the surface of the native MDCK cell line showed that the apical cell border is characterized by finger-like projections (microvilli) and close contact between the juxtaposed cells. Fracture faces of the apical plasma membranes displayed the characteristic organization of TJ:linear strands interconnected to form a junctional complex of anastomosing ridges on the protoplasmic face (PF) and linear depressions or grooves on the exoplasmic face (EF). Two to three parallel strands formed by linear rows encircle, without interruption, the apical cell periphery (Figure 6A). A similar type of TJ linear strands was detected by freeze-fracture in MDCK cells expressing GFP-Rab13T22N (Figure 6B). Conversely, the MDCK cells expressing GFP-Rab13Q67L were characterized by increased tortuosity and overlapping of both lateral and apical cell borders with rather large interspaces between the adjoining plasma membranes. In many areas of the freeze-fractured plasma membranes the TJ strands were randomly assembled and appeared as pleomorphic clusters of anastomosing filaments. Surprisingly, the tight junctional structures running along the apical cell periphery did not form a continuous belt but rather a discontinuous series of stranded clusters (Figure 6C). Furthermore, in some areas, TJ strand clusters appeared as a loose meshwork that was not restricted to the apical region of the lateral membrane but extended along the lateral domain of cells expressing GFP-Rab13Q67L (Figure 6D).

Rab13Q67L Mutant Affects Claudin1 Localization

We next examined whether the alteration of TJ strand organization induced by Rab13Q67L mutant correlated with changes in the localization of occludin and claudin1, two TJ transmembrane proteins, and ZO-1, a peripheral TJ protein. For this purpose, MDCK clones were plated at high identical density, grown on filters for 3 d, and then processed for confocal microscopy. The confocal *x-y* sections showed prominent sharp ring-like structures of occludin and ZO-1 on the lateral membrane between neighboring cells. The distribution of these proteins was very similar in parental as well as in MDCK expressing GFP, GFP-Rab13T22N (Figure 7). We found that occludin is also associated with the lateral membrane and is not restricted to TJ. Overexpression of GFP-Rab13Q67L affected slightly the localization of ZO-1 but did not apparently affect that of occludin. In control cells (MDCK, MDCK-GFP), claudin1 hexagonal staining characteristic of junctional complexes was detected. Some claudin1-positive vesicular structures were observed. Claudin1 distribution in GFP-Rab13T22N–expressing cells appeared similar to those observed in control cells. In GFP-Rab13Q67L–expressing cells, claudin1 was weakly detected at cell–cell junctions on the lateral plasma membrane; most of claudin1 immunoreactivity was observed in the cytoplasm (Figure 7), suggesting that the activated GFP-Rab13Q67L altered the distribution of claudin1.

Junctional complexes are dynamic structures that are continuously assembled/disassembled in vivo. To analyze whether GFP-Rab13Q67L interferes with the recruitment to the lateral membrane of claudin1, confluent MDCK clones were incubated in low calcium medium for 15 h to dissociate cell–cell junctions. Subsequent restoration of physiological level of calcium results in the synchronous de novo assembly of adherens and tight junctions. The localization of claudin1, ZO-1, and E-cadherin was analyzed by immunofluorescence at 0, 2, 4, and 15 h after induction of cell–cell contacts. In control cells as well as cells expressing GFP-Rab13 T22N and Q67L mutants, removal of calcium from the medium resulted in the dissociation of cell–cell junctions and redistribution of E-cadherin, ZO-1, and claudin1 (Figure 8). Membrane dissociation of these proteins was reversible. Within 2 h after readdition of calcium to the culture medium, the intracellular E-cadherin staining decreased, and the plasma membrane labeling increased at cell–cell contacts. Although the kinetics of membrane localization of this protein appeared similar in control cells and in MDCK expressing GFP-Rab13 T22N and Q67L mutants (Figure 8A), we cannot rule out that GFP-Rab13Q67L might be involved in the targeting of E-cadherin. Identical pattern of recovery of claudin1 and ZO-1 was observed in MDCK expressing GFP and GFP-Rab13T22N (Figure 8, B and C). Expression of GFP-Rab13Q67L slightly delayed the recruitment of ZO-1 to the cell–cell junctions. Interestingly, plasma membrane recruitment of claudin1 in MDCK expressing GFP-Rab13Q67L was delayed. Within 4 h after readdition of calcium, most of the claudin1 staining was not detected at the plasma membrane and was still observed in the cytoplasm. Fifteen hours after calcium add-back, claudin1 was detected at the lateral membrane (Figure 8C). The recruitment of GFP-Rab13Q67L protein to the plasma membrane occurred earlier (2 h) during cell–cell contact reassembly (supplementary material). These data confirm that the expression of GFP-Rab13Q67L delayed claudin1 recruitment and to a lesser extent that of ZO-1 to the lateral membrane during junctional complex assembly and did not efficiently impair the localization to the plasma membrane of E-cadherin.

Detergent Solubility of Tight Junction Proteins

In epithelial cells, TJ membrane proteins partitioned in two distinct pools: a Triton X-100–insoluble fraction that could represent a specific pool associated with TJ membrane microdomain (Nusrat *et al.*, 2000) and a TX-100 soluble pool that may represent the non–TJ-associated pool. Because these two pools are likely functionally distinct, we analyzed whether there were any differences in the Triton X-100 extractability of the occludin and claudin1 from cells expressing GFP or GFP-Rab13 mutants. Figure 9 shows the distribution of TJ proteins occludin and claudin1 in Triton X-100–soluble and –insoluble fractions. The Triton X-100 insolubility of occludin in cells expressing GFP, GFP-Rab13T22N, and GFP-Rab13Q67L was similar. We did not detect any change in the Triton X-100 extractability of clau-

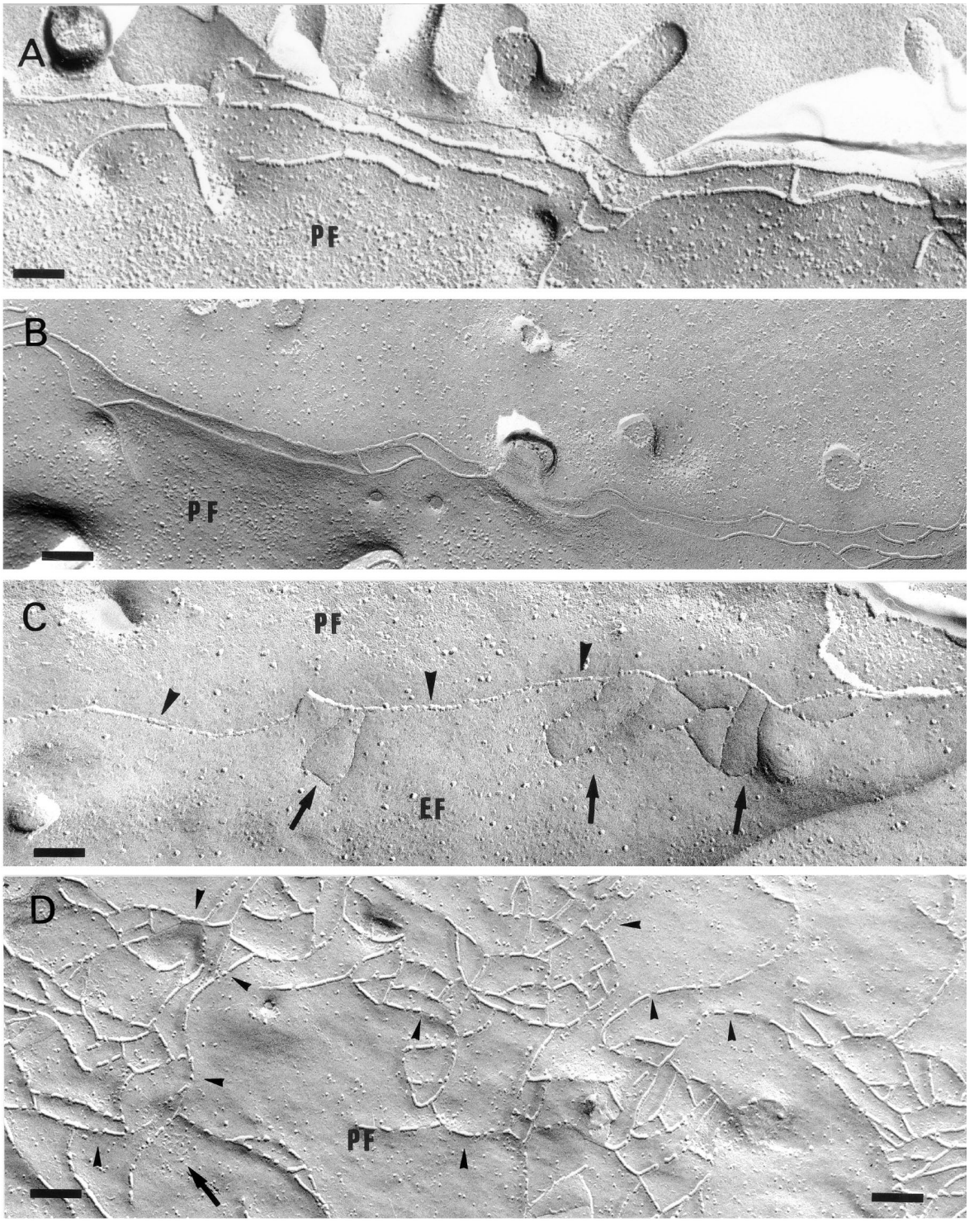

Figure 6. Freeze-fracture replica images of TJ of (A) MDCK, (B) MDCK expressing GFP-Rab13T22N and (C and D) GFP-Rab13Q67L cells grown for 3 d. The apical cell border is characterized by finger-like projections. (A and B) TJ linear and continuous strands occupy the apical zone of the lateral membrane. PF, protoplasmic fracture face; EF, exoplasmic fracture face. Bar, 100 nm. (C) The TJ domain comprises clusters of furrows on EF (arrows), interconnected by one single particulate strand running along the intermembrane space (arrowhead). (D) Note that individual strands are fragmented, and a subunit pattern is visible (arrowheads). The arrow points to a cluster of particulate entities segregated from the strands. Bar, 150 nm.

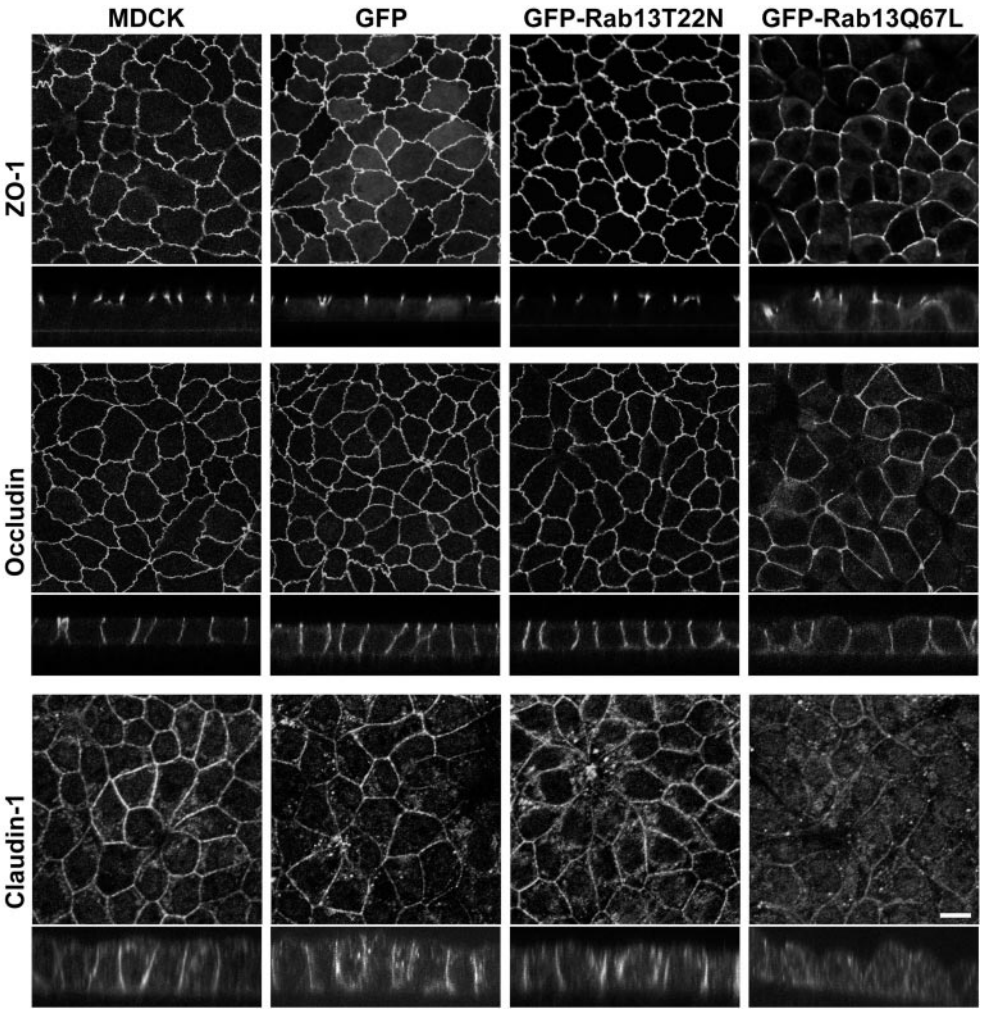

Figure 7. Confocal immunofluorescence localization of ZO-1, occludin, and claudin1 in MDCK cells, MDCK expressing GFP, GFP-Rab13T22N, and GFPRab13Q67L. Cells were grown on filters for 3 d and processed for immunofluorescence with either anti-occludin, anti-ZO-1, and anti-claudin1 antibodies as described in MATERIALS AND METHODS. Images of one focal section across the tight junction and *X–Z* views showed ZO-1, occludin, and claudin1 immunolabeling. Bar, 10 μm.

din1 in MDCK expressing GFP or GFP-Rab13T22N. However, expression of GFP-Rab13Q67L coincided with a decrease (40%) in claudin1 TX-100–insoluble pool. As shown in Figure 9B, the insoluble/soluble ratio of claudin1 in GFP-Rab13Q67L cells was lower than those in GFP or GFP-Rab13T22N cells. This suggests that the protein was poorly associated with TJ membranes.

DISCUSSION

Our results demonstrate that expression of GFP-Rab13Q67L but not the inactive GFP-Rab13T22N mutant alters the distribution of the tight junction membrane protein, claudin1

As a consequence, TJ formed in MDCK cells expressing GFP-Rab13GTP are structurally disorganized and functionally leaky for small tracers despite being an effective barrier to ion flow

To investigate the role of Rab13 in epithelial TJ organization, we generated two Rab13 mutants, T22N and Q67L. Rab13 mutants were expressed in MDCK cells as GFP-Rab13 fusion proteins. Our finding that GFP-Rab13 WT and Q67L are localized on the lateral membrane including TJ in MDCK cells is different from data on Caco-2 cells reported earlier by us. Immunofluorescence labeling of polarized intestinal Caco-2 cells showed that Rab13 colocalized with ZO-1 (Zahraoui *et al.*, 1994). Unfortunately, our attempts (including this work) to localize Rab13 by EM have failed. The precise localization of Rab13 might be different in polarized MDCK and Caco-2 cells. We note that in MDCK cells, as in Caco-2 cells, the formation of cell–cell contact is required for the recruitment of Rab13 to the plasma membrane. It is possible that the antipeptide we used earlier (Zahraoui *et al.*, 1994) recognized only the TJ associated pool of Rab13. Interestingly, depending on the antibodies used, claudins are not restricted to TJ but can be found on the lateral membrane (Rahner *et al.*, 2001). Recently, Yeaman *et al.* (2001) used a panel of monoclonal antibodies to Sec6 and Sec8 and found that some antibodies stained Sec6/s8 at cell–cell contact sites and others antibodies stained Sec6/s8 in a perinuclear compartment. The implication of this lateral distribution of GFP-Rab13 in MDCK cells is unclear. Perhaps, Rab13 has an additional function independent of TJ in MDCK cells. The presence of Rab13 in epithelial and fibroblast cells strengthens the notion that Rab13 may have additional role, independent of TJ, in cell surface polarization (Zahraoui *et al.*,

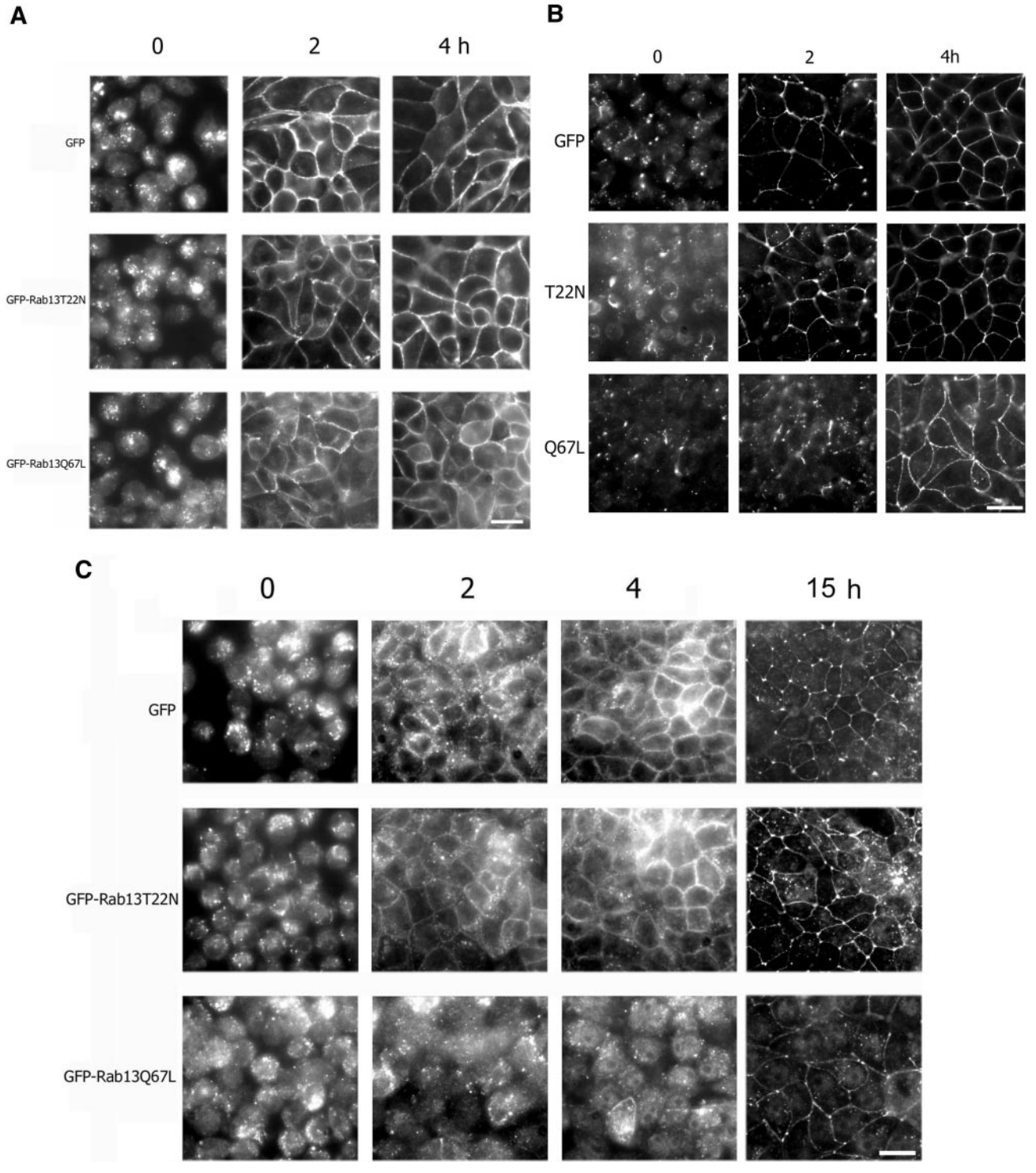

Figure 8. Expression of GFP6Rab13Q67L delays the recruitment of claudin1 to the plasma membrane during TJ assembly after calcium switch. Confluent MDCK expressing GFP, GFP-Rab13T22N, and GFP-Rab13Q67L were incubated in low calcium medium for 15 h and then reincubated in normal medium for 0, 2, and 4 h and stained with (A) anti-E-cadherin, (B) anti-ZO-1, and (C) anti-claudin1 antibodies. Within 2 h after readdition of calcium to the culture medium, E-cadherin accumulated in the lateral membrane in control cells and in MDCK expressing GFP-Rab13 T22N and Q67L mutants. A similar pattern of plasma membrane recruitment of ZO-1 and claudin1 was observed in MDCK expressing GFP and GFP-Rab13T22N. Plasma membrane recruitment of claudin1 in MDCK expressing GFP-Rab13Q67L was delayed but recruitment of ZO-1 is only slightly affected. Bar, 10 μm.

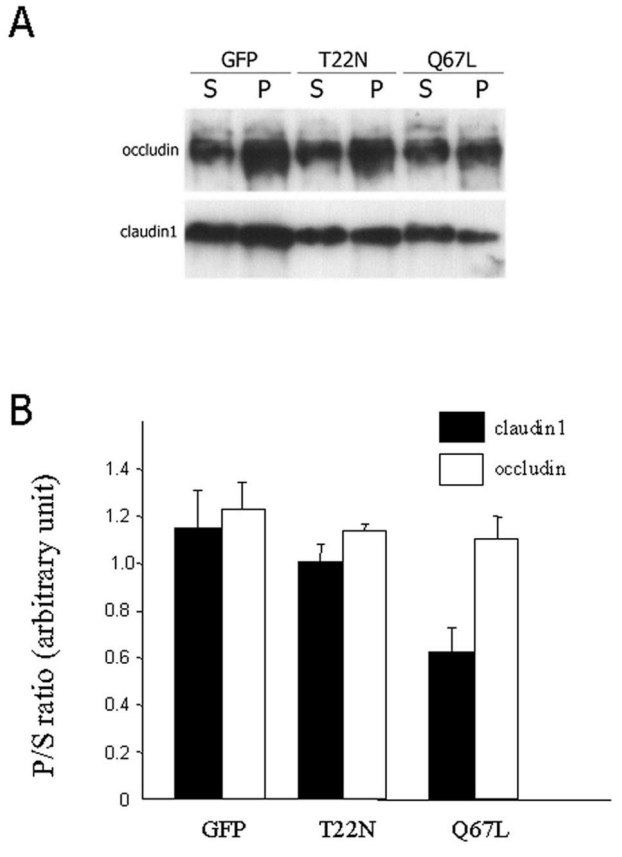

Figure 9. Triton X-100 extractability of TJ proteins occludin and claudin1 in MDCK cells expressing GFP, GFP-Rab13T22N, and GFP-ab13Q67L. Cells were grown for 3 d, extracted in buffer containing 0.5% Triton X-100 for 20 min at 0°C, and centrifuged. Proteins in equal amounts of Triton X-100–soluble (S) and –insoluble (P) fractions were separated by SDS-PAGE, and transferred to nitrocellulose filters. The upper and lower parts of the filters were probed with anti-occludin and anti-claudin1 antibodies, respectively. Results shown are representative of three experiments. (B) Quantification of three independent experiments performed as in A. After blotting, soluble and insoluble occludin and claudin1 protein bands were quantified using the Scion image program (NIH image, Rockville, MD) and Microsoft Excel software. The insoluble (P)/soluble (S) ratio was calculated (mean ± SEM). Note that the claudin1 P/S ratio from MDCK expressing GFP-Rab13Q67L was lower than those from the other cells.

1994). Alternatively, the lateral distribution of GFP-Rab13 might represent a pool that can be recruited into TJ to acutely alter the localization of claudin1 and disturb the paracellular diffusion properties of TJ in response to physiological signals.

TJ Gate and Fence Functions Are Impaired by the Activated GFP-Rab13

Measurement of TER and tracer flux across the TJ was used to monitor the formation of the TJ barrier during TJ assembly. Although GFP-Rab13 WT and T22N are weakly expressed, they affected TER recovery. We suggest that a weak expression of the two proteins is likely sufficient to affect TER development in these cells. We found that neither inactive Rab13T22N, nor active Rab13Q67L mutants could significantly affect steady state TER. However, when TER is measured during course of TJ formation, it indicated that expression of GFP-Rab13Q67L caused a significant delay in TER development. The TER lag induced by active GFP-Rab13Q67L and the fact that its expression did not affect TER steady state strongly suggested that Rab13 acts specifically during the assembly of TJ. Analyses of tracer (mannitol, 4 and 40 kDa dextran) movement through TJ revealed that expression of inactive GFP-Rab13T22N reduced the diffusion of the small tracers. In contrast, expression of GFP-Rab13Q67L resulted in a significant increase in paracellular flux. These data indicated that constitutively active Rab13 reduced the tightness of the seal between neighboring cells. Claude (1978) suggested the existence of series of compartmentalized aqueous channels that fluctuate between closed and open states within the TJ strand network. According to this model, flux measurements of tracers reflect the sum of fluxes through TJ pores over a period of time, whereas TER is an instantaneous indicator of permeability. Consequently, the relationship between TER and paracellular flux could be nonlinear (Balda *et al.*, 1996, Madara, 1998; McCarthy *et al.*, 2000). This could explain the functional dissociation of paracellular permeability from TER in cells expressing GFP-Rab13 mutants. In addition to disrupting TJ gate function, we found that the expression of GFP-Rab13Q67L altered the localization of the apical, gp114, and the basolateral, gp58, membrane proteins as well as the lateral diffusion of a lipid, BODIPY-sphingosylphosphorylcholin/BSA. In contrast, the expression of the inactive mutant (Rab13T22N) did not alter the localization of gp58 and gp114 proteins or the diffusion of fluorescent lipid. Thus, the structural organization of TJ responsible for the intramembrane fence and the paracellular permeability seal appear to be altered in GFP-Rab13Q67L cells. It is possible that the partial mislocalization of gp114 and gp58 in GFP-Rab13Q67L cells might not be due to the disruption of TJ fence per se but to a mechanism involving GFP-Rab13GTP in the maintenance of apico-basolateral polarity in epithelial cells.

One of the most striking observations made in this study is the formation of aberrant strands along the lateral surface of cells expressing GFP-Rab13Q67L but not GFP-Rab13T22N. The TJ of cells expressing the GFP-Rab13Q67L mutant appeared as a fragmented and clustered assembly of anastomotic filaments. Our data suggest that TJ strand organization in GFP-Rab13Q67L cells is sufficiently disrupted to permit lipids to diffuse through the TJ barrier and to alter the organization of apical and basolateral membrane proteins. Although we observed a reduction in tracer diffusion through the TJ, we did not observe any change in TJ strand organization in GFP-Rab13T22N cells, suggesting that an efficient functional paracellular barrier may not require several intramembrane strands.

Rab13 Is Required for TJ Assembly

TJ strands appear to be formed by homo- or heteropolymers of claudins and occludin, which pair laterally with those in apposing membranes to seal the paracellular space between adjacent cells. These integral membrane proteins are linked to the underlying actin cytoskeleton via cytosolic proteins

such as ZO-1 (Tsukita and Furuse, 1999, 2000). At present it is not clear how TJ protein organization might affect TJ barrier functions. Although occludin is a key component of TJ strands (Furuse *et al.*, 1993; Balda *et al.*, 1996; Wong and Gumbiner, 1997), recent work suggests that it is not sufficient to generate TJ strands. For example, visceral endoderm cells in which the occludin gene is knocked out still develop a normal TJ strand network (Saitou *et al.*, 1998). Several reports indicate that claudins are required for the generation of TJ strands and for the establishment of the paracellular diffusion barrier (Furuse *et al.*, 1998a; Tsukita and Furuse, 2000). Expression of claudin1 and 2 in fibroblasts lacking TJ induces the formation of strands that are morphologically similar to the epithelial TJ strands (Furuse *et al.*, 1998b). Analysis of OSP/claudin11-deficient mice reveals the absence of TJ strands in myelin sheets of oligodendrocytes and sertoli cells and paracellin1/claudin16 mutations cause renal Mg^{2+} wasting (Gow *et al.*, 1999; Simon *et al.*, 1999). Our data indicate that expression of GFP-Rab13Q67L dramatically altered the distribution of claudin1 but not significantly that of occludin. In these cells, ZO-1 exhibited only a slight distribution change and still formed a continuous junctional ring, suggesting that its localization is not determined only by Rab13. We suggest that alteration of TJ barrier functions in cell expressing GFP-Rab13Q67L is due to the abnormal organization of claudin1, and to a lesser extent to that of ZO-1, in the TJ area. Moreover, our data revealed that the claudin1 Triton X-100-insoluble pool that might represent the TJ-associated fraction was dramatically reduced in MDCK expressing GFP-Rab13Q67L. Although the mechanisms involved are not known, we speculate that alteration of the dynamics of claudin1 association to/dissociation from TJ membrane by GFP-Rab13Q67L may perturb the structural and functional properties of the intramembrane strands.

Interestingly, calcium switch experiments indicated that the expression of GFP-Rab13Q67L mutant delayed the recruitment of claudin1 to the plasma membrane, strengthening the notion that Rab13 may play an important role in coordinating the recruitment of claudin1/ZO-1 to specific domains on the lateral membrane. Unfortunately, we did not detect any interaction between Rab13 and claudin1/ZO-1, suggesting that the effect of Rab13 on both proteins is likely indirect. Probably because of the lack of classical ectodomains, we failed to biotinylate claudin1 and were therefore unable to show whether GFP-Rab13Q67L inhibited the transport of claudin1 to the plasma membrane. It has been suggested that E-cadherin mediates the translocation of ZO-1 that recruits other TJ proteins required for functional assembly of TJ (Rajasekaran *et al.*, 1996; Troxell *et al.*, 2000). The effect of GFP-Rab13Q67L on TJ does not appear to be mediated by E-cadherin, because overexpression of active GFP-Rab13 does not significantly impair the recruitment of E-cadherin to the lateral membrane. Rab proteins act in conjunction with a variety of protein effectors to regulate different steps of exocytic and endocytic pathways (Schimmoller *et al.*, 1998; Chavrier and Goud, 1999; Zerial and McBride, 2001). Accordingly, it is tempting to speculate that Rab13, in its GTP-bound and membrane bound form, recruits an effector (s) that inhibits the recruitment of claudin1 to the cell surface. Conversely, Rab13T22N (inactive form) unable to recruit the effector to the lateral membrane may favor the establishment of TJ gate and fence functions. Alternatively, it is also possible that in cells expressing the GTPase-deficient mutant, GFP-Rab13Q67L, claudin1 is transported to the cell surface but is reinternalized because it is not incorporated into TJ. The opposite effects of the GFP-Rab13 Q67L and T22N mutants on TJ suggest that Rab13GTP is required before claudin1 recruitment, whereas GTP hydrolysis by Rab13 occurs after claudin1 recruitment, inactivating Rab13 and allowing claudin1 incorporation into TJ. So, our data indicate that Rab13 may play an important role in the assembly of TJ and thus in the establishment of polarity in epithelial cells.

ACKNOWLEDGMENTS

The authors are grateful to Dr. J. Plastino for critical reading of the manuscript. This work was supported by grants from CNRS, Institut Curie, and the Association pour la Recherche sur le Cancer (ARC 5789 to A.Z). A-M.M. and R.P. are recipients of fellowships from the ARC and Institut Curie, respectively.

REFERENCES

Anderson, J.M., Van Itallie, C.M., Peterson, M.D., Stevenson, B.R., Carew, E.A., and Mooseker, M.S. (1989). ZO-1 mRNA and protein expression during tight junction assembly in Caco-2 cells. J. Cell Biol. *109*, 1047–1056.

Balda, M.S., Gonzalez-Mariscal, L., Matter, K., Cereijido, M., and Anderson, J.M. (1993). Assembly of the tight junction: the role of diacylglycerol. J. Cell Biol. *123*, 293–302.

Balda, M.S., and Matter, K. (2000). The tight junction protein ZO-1 and an interacting transcription factor regulate ErbB-2 expression. EMBO J. *19*, 2024–2033.

Balda, M.S., Whitney, J.A., Flores, C., Gonzalez, S., Cereijido, M., and Matter, K. (1996). Functional dissociation of paracellular permeability and transepithelial electrical resistance and disruption of the apical-basolateral intramembrane diffusion barrier by expression of a mutant tight junction membrane protein. J. Cell Biol. *134*, 1031–1049.

Bucci, C., Parton, R.G., Mather, I.H., Stunnenberg, H., Simons, K., Hoflack, B., and Zerial, M. (1992). The small GTPase rab5 functions as a regulatory factor in the early endocytic pathway. Cell *4,* 715–728.

Chavrier, P., and Goud, B. (1999). The role of ARF and Rab GTPases in membrane transport. Curr. Opin. Cell Biol. *11*, 466–475.

Claude, P. (1978). Morphological factors influencing transepithelial permeability: a model for the resistance of the zonula occludens. J. Membr. Biol. *39*, 219–232.

Cordenonsi, M., D'Atri, F., Hammar, E., Parry, D.A., Kendrick-Jones, J., Shore, D., and Citi, S. (1999). Cingulin contains globular and coiled-coil domains and interacts with ZO-1, ZO-2, ZO-3, and myosin. J. Cell Biol. *147*, 1569–1582.

Dunia, I., Recouvreur, M., Nicolas, P., Kumar, N.M., Bloemendal, H., Benedetti, E.L. (2001). Sodium dodecyl sulfate-freeze-fracture immunolabeling of gap junctions. Methods Mol. Biol. *154*, 33–55.

Echard, A., Jollivet, F., Martinez, O., Lacapere, J.J., Rousselet, A., Janoueix-Lerosey, I., and Goud, B. (1998). Interaction of a Golgi-associated kinesin-like protein with Rab6. Science *279*, 580–585.

Fujimoto, K. (1997). SDS-digested freeze-fracture replica labeling electron microscopy to study the two-dimensional distribution of integral membrane proteins and phospholipids in biomembranes: practical procedure, interpretation and application. Histochem. Cell Biol. *107,* 87–96.

Furuse, M., Fujita, K., Hiiragi, T., Fujimoto, K., and Tsukita, S. (1998a). Claudin-1 and -2: novel integral membrane proteins local-

izing at tight junctions with no sequence similarity to occludin. J. Cell Biol. *141*, 1539–1550.

Furuse, M., Hirase, T., Itoh, M., Nagafuchi, A., Yonemura, S., and Tsukita, S. (1993). Occludin: a novel integral membrane protein localizing at tight junctions. J. Cell Biol. *123*, 1777–1788.

Furuse, M., Sasaki, H., Fujimoto, K., and Tsukita, S. (1998b). A single gene product, claudin-1 or -2, reconstitutes tight junction strands and recruits occludin in fibroblasts. J. Cell Biol. *143*, 391–401.

Gow, A., Southwood, C.M., Li, J.S., Pariali, M., Riordan, G.P., Brodie, S.E., Danias, J., Bronstein, J.M., Kachar, B., and Lazzarini, R.A. (1999). CNS myelin and sertoli cell tight junction strands are absent in Osp/claudin-11 null mice. Cell *99*, 649–659.

Grindstaff, K.K., Yeaman, C., Anandasabapathy, N., Hsu, S.C., Rodriguez-Boulan, E., Scheller, R.H., and Nelson, W.J. (1998). Sec6/8 complex is recruited to cell-cell contacts and specifies transport vesicle delivery to the basal-lateral membrane in epithelial cells. Cell *93*, 731–740.

Gumbiner, B., Stevenson, B., and Grimaldi, A. (1988). The role of the cell adhesion molecule uvomorulin in the formation and maintenance of the epithelial junctional complex. J. Cell Biol. *107*, 1575–1587.

Huber, L.A., Pimplikar, S., Parton, R.G., Virta, H., Zerial, M., and Simons, K. (1993). Rab8, a small GTPase involved in vesicular traffic between the TGN and the basolateral plasma membrane. J. Cell Biol. *123*, 35–45.

Itoh, M., Furuse, M., Morita, K., Kubota, K., Saitou, M., and Tsukita, S. (1999). Direct binding of three tight junction-associated MAGUKs, ZO-1, ZO-2, and ZO-3, with the COOH termini of claudins. J. Cell Biol. *147*, 1351–1363.

Kato, M., Sasaki, T., Ohya, T., Nakanishi, H., Nishioka, H., Imamura, M., and Takai, Y. (1996). Physical and functional interaction of rabphilin-3A with a-actinin. J. Biol. Chem. *271*, 31775–31778.

Louvard, D. (1980). Apical membrane aminopeptidase appears at site of cell-cell contact in cultured kidney epithelial cells. Proc. Natl. Acad. Sci. USA *77*, 4132–4136.

Madara, J.L. (1998). Regulation of the movement of solutes across tight junctions. Annu. Rev. Physiol. *60*, 143–159.

McCarthy K.M., Francis F.A., McCormack J.M., Lai J., Rogers R.A., Skare I.B., Lynch R.D., and Schneeberger, E.E.. (2000). Inducible expression of claudin1-myc but not occludin-VSV results in aberrant tight junction strand formation in MDCK cells. J. Cell Sci. *113*, 3387–3398.

Nielsen, E., Severin, F., Backer, J.M., Hyman, A.A., and Zerial, M. (1999). Rab5 regulates motility of early endosomes on microtubules. Nat. Cell Biol. *1*, 376–382.

Nusrat, A., Parkos, C.A., Verkade, P., Foley, C.S., Liang, T.W., Innis-Whitehouse, W., Eastburn, K.K., and Madara, J.L. (2000). Tight junctions are membrane microdomains. J. Cell Sci. *113*, 1771–1781.

Peränen, J., Auvinen, P., Virta, H., Wepf, R., and Simons, K. (1996). Rab8 promotes polarized membrane transport through reorganization of actin and microtubules in fibroblasts. J. Cell Biol. *135*, 153–157.

Rajasekaran, A.K., Hojo, M., Huima, T., and Rodriguez-Boulan, E. (1996). Catenins and zonula occludens-1 form a complex during early stages in the assembly of tight junctions. J. Cell Biol. *132*, 451–463.

Rahner, C., Mitic, L.L., and Anderson, J.M. (2001). Heterogeneity in expression and subcellular localization of claudins 2, 3, 4, and 5 in the rat liver, pancreas, and gut. Gastroenterology *120*, 411–422.

Ren, M., Zeng, J., De, L., Chiarandini, C., Rosenfeld, M., Adesnik, M., and Sabatini, D.D. (1996). In its active form, the GTP-binding protein rab8 interacts with a stress-activated protein kinase. Proc. Natl. Acad. Sci. USA *93*, 5151–5155.

Saitou, M., Fujimoto, K., Doi, Y., Itoh, M., Fujimoto, T., Furuse, M., Takano, H., Noda, T., and Tsukita, S. (1998). Occludin-deficient embryonic stem cells can differentiate into polarized epithelial cells bearing tight junctions. J. Cell Biol. *141*, 397–408.

Schimmoller, F., Simon, I., and Pfeffer, S.R. (1998). Rab GTPases, directors of vesicle docking. J. Biol. Chem. *273*, 22161–22164.

Sheth, B., Fontaine, J., Ponza, E., McCallum, A., Page, A., Citi, S., Louvard, D., Zahraoui, A., and Fleming, T.P. (2000). Differentiation of the epithelial apical junctional complex during mouse preimplantation development: a role for rab13 in the early maturation of the tight junction. Mech. Dev. *97*, 93–104.

Simon D.B., Lu, Y., Choate, K.A., Velazquez, H., Al-Sabban, E., Praga, M., Casari, G., Bettinelli, A., Colussi, G., Rodriguez-Soriano, J., McCredie, D., Milford, D., Sanjad, S., and Lifton, R.P. (1999). Paracellin-1, a renal tight junction protein required for paracellular Mg2+ resorption. Science *285*, 103–106.

Stenmark, H., Vitale, G., Ullrich, O., and Zerial, M. (1995). Rabaptin-5 is a direct effector of the small GTPase Rab5 in endocytic membrane fusion. Cell *83*, 423–432.

Troxell, M.L., Gopalakrishnan, S., McCormack, J., Poteat, B.A., Pennington, J., Garringer, S.M., Schneeberger, E.E., Nelson, W.J., and Marrs, J.A. (2000). Inhibiting cadherin function by dominant mutant E-cadherin expression increases the extent of tight junction assembly. J. Cell Sci. *113*, 985–996.

Tsukita, S., and Furuse, M. (1999). Occludin and claudins in tight-junction strands: leading or supporting players? Trends Cell Biol. *9*, 268–273.

Tsukita, S., and Furuse, M. (2000). Pores in the wall: claudins constitute tight junction strands containing aqueous pores. J. Cell Biol. *149*, 13–16.

Weber E., Berta, G., Tousson, A., St John, P., Green, M.W., Gopalokrishnan, U., Jilling, T., Sorscher, E.J., Elton, T.S., and Abrahamson, D.R. (1994). Expression and polarized targeting of a rab3 isoform in epithelial cells. J. Cell Biol. *125*, 583–594.

White, J., Johannes, L., Mallard, F., Girod, A., Grill, S., Reinsch, S., Keller, P., Tzschaschel, B., Echard, A., Goud, B., and Stelzer, E.H. (1999). Rab6 coordinates a novel Golgi to ER retrograde transport pathway in live cells. J. Cell Biol. *147*, 743–760.

Wittchen, E.S., Haskins, J., and Stevenson, B.R. (1999). Protein interactions at the tight junction. Actin has multiple binding partners, and ZO-1 forms independent complexes with ZO-2 and ZO-3. J. Biol. Chem. *274*, 35179–35185.

Wong, V., and Gumbiner, B.M. (1997). A synthetic peptide corresponding to the extracellular domain of occludin perturbs the tight junction permeability barrier. J. Cell Biol. *136*, 399–409.

Yeaman, C., Grindstaff, K.K., Wright, R.J., and Nelson, W.J. (2001). Sec6/8 complexes on trans-Golgi network and plasma membrane regulate late stages of exocytosis in mammalian cells. J. Cell Biol. *155*, 593–604.

Zahraoui, A., Joberty, G., Arpin, M., Fontaine, J.J., Hellio, R., Tavitian, A., and Louvard, D. (1994). A small rab GTPase is distributed in cytoplasmic vesicles in non polarized cells but colocalizes with the tight junction marker ZO-1 in polarized epithelial cells. J. Cell Biol. *124*, 101–115.

Zahraoui, A., Louvard, D., and Galli, T. (2000). Tight junction, a platform for trafficking and signaling protein complexes. J. Cell Biol. *151*, F31–F36.

Zerial, M., and McBride, H. (2001). Rab proteins as membrane organizers. Nat. Rev. Mol. Cell. Biol. *2*, 107–119.